LIQUEFACTION POTENTIAL & POST EARTHQUAKE STABILITY ASSESSMENT

Project ID: CEEn_2016CPST_013

by

H2J Engineering

Project Mentor: Tyler Coutu

Team Lead: Heidi Decayanan

Equipment Specialist: Joshua Peterson

Operations Management: Joel Yellowhorse

A Capstone project submitted to

Robert Snow from

Department of Civil and Environmental Engineering

Ira A. Fulton College of Engineering and Technology

Brigham Young University

April 19, 2017

<u>**Table of Contents**</u>

Executive Summary

Currently the factor of safety calculations and cross sections are completed. Parameters concerning the general soil characteristics have been gathered and tabulated. The conclusion of the project has identified several liquefiable layers at the site that will pose potential hazard zones in the event of an earthquake. Several cross sections have been completed to illustrate the location and susceptibility of the liquefiable layers for the final analysis and report. Analysis was done using principles from studies done by Idriss and Boulanger on a deterministic level for several different earthquake scenarios. This information can be used to make an informed decision to remediate potential hazards to the bridge and adjoining structure.

Introduction

This Project has proved to be a very straightforward example of earthquake liquefaction potential. The boring logs that were presented for the analysis provide sufficient information to determine the general soil characteristics. Using data from the USGS on earthquake intensities and these soil profiles this information can then be used to make an accurate summary of the soil strength and expected loading. This is basic soil mechanics and was not too difficult to perform. Most of the researching was centered on how to take this data and make an accurate prediction of the factor of safety under an average earthquake. The tools that were researched and built to help with this prediction are featured in the body of this report.

Report

To get an accurate picture and to make an effective presentation of the ground underneath the bridge and road structure it was necessary to draw AutoCAD representations of the expected soil layers. The general layout of the soil can be seen in the figure and can be used to visualize what a potential liquefaction scenario might cause and what surface displacements might result. Layers were generally taken to be continuous and changed linearly throughout the span of the sampling area. Very few abrupt changes were necessary to make an adequate picture.

These three profiles will show an overall view of all the data collected and give a 3-dimensional perspective to this analysis. A diagram showing the layout of these profiles superimposed on the map provided by AECOM of the boring logs is shown below in Figure 1. These locations were chosen because they provide cross sections at both ends and down the center of the highway. This way soil behavior can be accounted for in multiple directions.

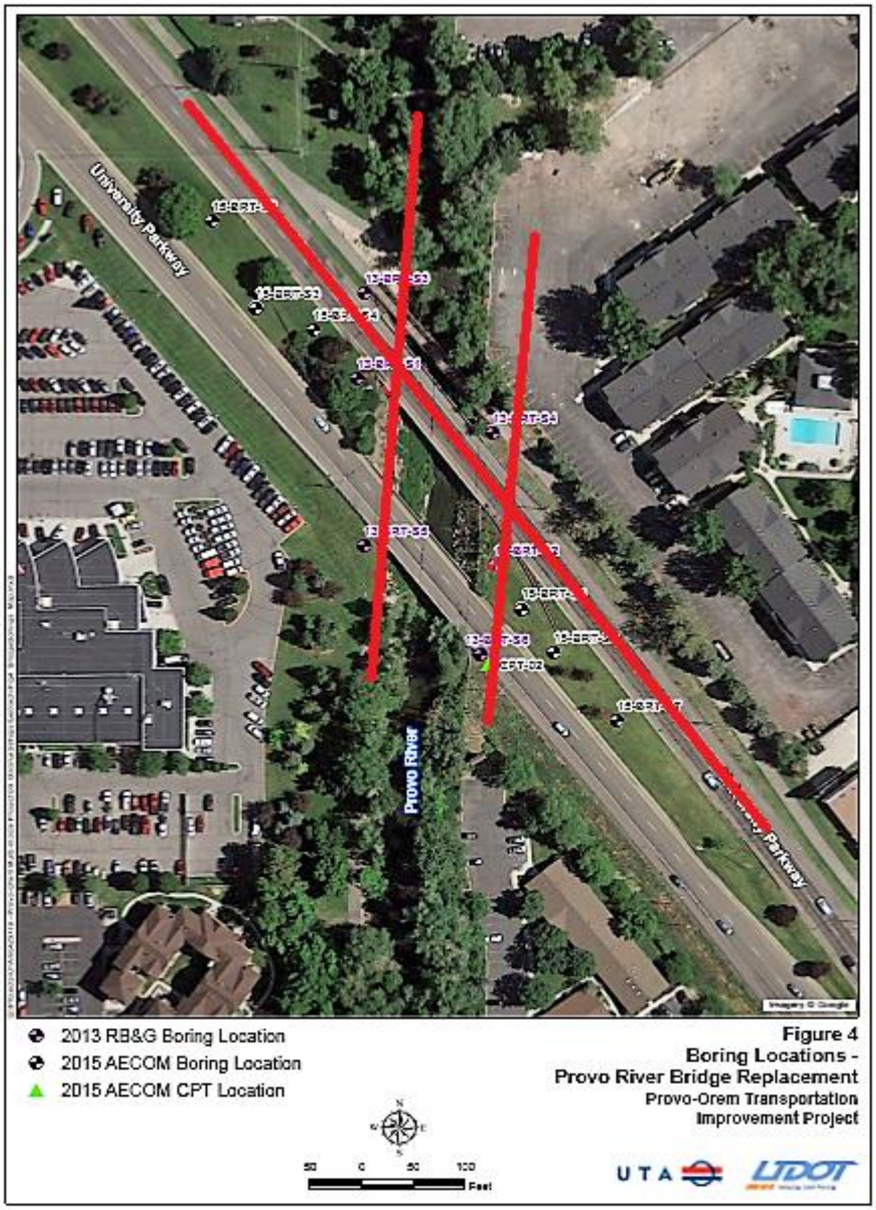

Figure 1. Aerial view of cross sections layouts for final report.

Most the research that has been done on this project centers around the calculations for factors of safety against liquefaction. These factors of safety allow us to know exactly how likely it is that a specific layer in the soil will undergo liquefaction during a given earthquake. To better understand the process necessary to predict the behavior of soil under earthquake conditions a deterministic approach was used. This means that all parameters for earthquake intensity are assumed by studying an average earthquake and then from that the factors of safety for each soil layer were found. To perform this analysis equations developed by Idriss and Boulanger were used as well as a series of commonly used correlations.

For each layer of soil the information on the $(N_1)_{60}$ blow counts and a general description of the soil were tabulated. Using the blow counts both the cyclic resistance ratio and the average density for each soil type was correlated, again using work by Idriss and Boulanger. Using the density of the soil and the water table level the effective normal stress on the soil could then be calculated throughout the area of interest. These numbers give an idea of the strength of the soil in resisting an earthquake. Data concerning an actual earthquake that might occur can be obtained from the USGS geohazards web site. Assuming a 475 year event, a 1039 year event and a 2475 year event the peak ground acceleration for the area could then be determined. This gives the strength of the earthquake that is expected to happen every 50 years. After understanding both the strength of the soil as well as the strength of the earthquake a factor of safety can then be correlated using the following equation.

$$FS_{Liq} = \frac{CRR_{M,\sigma' v}}{CSR} = \frac{CRR \cdot MSF \cdot K_\sigma \cdot K_\alpha}{0.65 \frac{a_{\max}}{g} \frac{\sigma_v}{\sigma_v'} (r_d)}$$

In this equation FS = factor of safety, CRR = cyclic resistance of the soil, CSR = cyclic stress caused by the earthquake, MSF = magnitude of the earthquake, a_{max} = the peak acceleration caused by the earthquake, σ'_v = effective stress in the soil, σ_v = normal stress in the soil, g = acceleration of gravity, r_d = distance below the surface of each soil layer, and K_σ and K_α are the initial stress states of the soil. For the two K values K_α is assumed to be 1 and K_σ can be correlated from the effective stress in the soil and the number of blows necessary to penetrate it.

Table 1 shows an example of the spreadsheets that were designed to perform the calculations for this analysis. Generally, layers that have a factor of safety greater than 2 are safe while factors of safety between 2 and 1 indicate that the soil is close to liquefying and factors below 1 show that the soil has already liquefied. Soils that have generally been known never to liquefy are discounted in the analysis since they generally produce extremely high values that do not necessarily reflect the strength of the soil. The USGS reported a peak ground acceleration of almost 5 ft/s^2 for a magnitude 7.5 earthquake in the Provo area. This would cause significant damage in the area and may even cause damage to the road and the bridge spanning the area of interest independent of damage caused by liquefaction.

Table 1. Calculated values for soil layers at sample area 15-BRT-S2

Material	Depth (ft)	$(N_1)_{60}$	CRR	ρ	C_σ	K_σ	σ_v	$\sigma_{v'}$	FS
Gravel	4	24.7	0.283	129	0.161	1.10	516	516	6.8
SP(Sand)	6	43.2	13.7	104	0.300	1.10	749	749	219
Gravel	9	36.6	1.59	103	0.288	1.10	1060	1060	16.9
Gravel	11	47.4	113	128	0.300	1.10	1291	1291	989
Gravel	14	57.1	373544	132	-2.71	0.37	1681	1681	873288
Boulders	16	100	2.7332E+73	1	-0.152	0.98	1945	1820	NA
Sandy Silt	19	15.6	0.161	88	0.113	1.01	2275	1963	0.65
Sandy Silt	21	13.7	0.146	86	0.106	1.01	2449	2012	0.50
Silty Sand	23	25.1	0.292	100	0.163	1.00	2635	2073	0.88
Silt	26	10.2	0.119	85	0.093	1.00	2912	2163	0.30
Silt	29	21.0	0.219	91	0.139	0.99	3176	2240	0.46
Silt	31	7.5	0.101	84	0.084	0.99	3351	2290	0.19
Silt	34	38.5	2.61	94	0.300	0.97	3618	2370	4.25

We can see that the upper half of the soil is resistant to liquefaction while the sands and silts below the water table have a much higher susceptibility. One adjustment that was made later is that the $(N_1)_{60}$ values needed to be adjusted to their clean sand equivalents to give the best estimate possible for the correlations. This is among the final issues that still needed to be resolved.

The type of deterministic analysis shown above is limited because it does not provide a range of data but instead gives engineers a view of how a structure would react under a single set of earthquake conditions. A more effective approach would be to perform a performance based analysis of the soil. Certain computer programs exist that allow for engineers to model the behavior of soil under a wide range of loadings and conditions. This allows for trends in the results to be identified and for optimization of any design improvements.

Conclusion

After analyzing and compiling our data we have found that there are a number of locations with a potential for liquefication. Our data shows that the areas closer to the river exhibit more locations of potential liquefication. Our data also shows that with depth the amount of potentially liquefiable layers increases. These outcomes were both expected due to the known water table level at the river and from previous research. To illustrate the data cross-sectional representations were created. Figure 1 shows the soil cross sections that correspond to the boring logs. The green areas have a low potential for liquefication which corresponds to a high factor of safety. The yellow to red areas show the increase in liquefication potential. The yellow areas show a factor of safety just below 2 and the red areas show a factor of safety below 1.

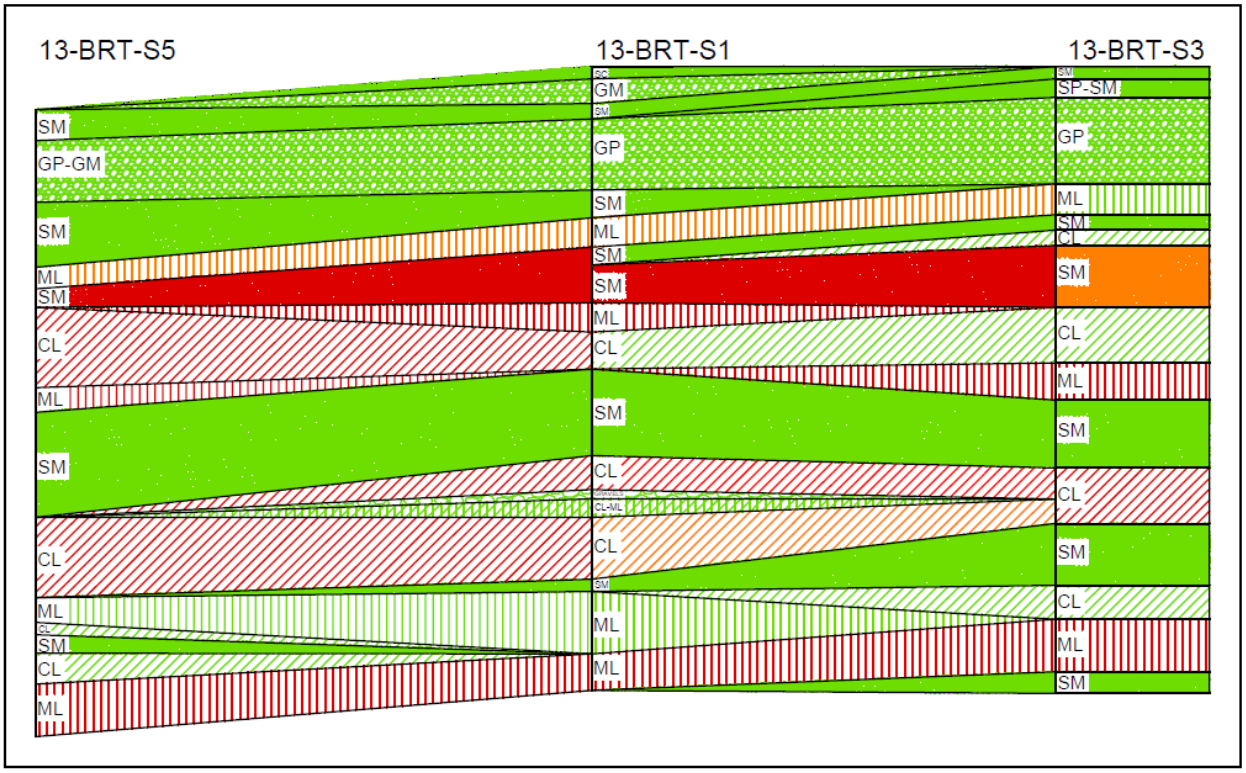

Figure 1. Soil cross-section 13-BRT-S5 to 13-BRT-S3

As shown in Figure 1 there are several layers that have a low potential to liquefication as well. Three additional cross-sections can be found in the attached appendix. See the attached boring log locations for cross-section reference locations.

Graphs were also created to illustrate the liquefication potential. Figure 2 shows the factor of safety with respect to depth for the boring log 13-BRT-S1 with a Peak ground acceleration (PGA) of 10% in 50 years.

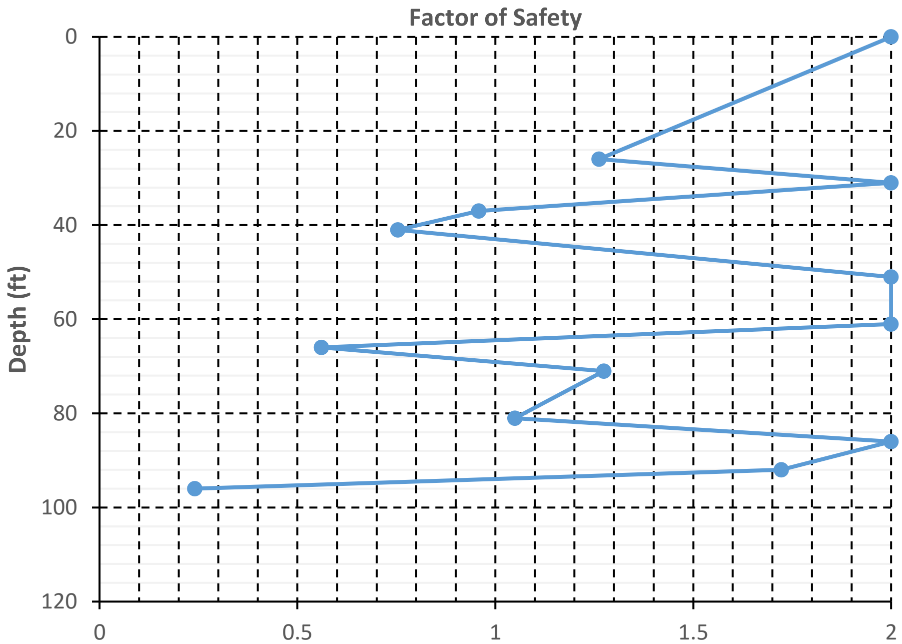

Figure 2. Factor of safety with respect to depth 13-BRT-S1, PGA 10%, 50 years

As you can see from the graph at the boring log labeled 13-BRT-S1 the areas of liquefication are sporadic throughout the soil layers. More graphs can be found in the attached appendix.

In conclusion, the layers of liquefication are shown in the attached figures and something will need to be done to sustainably support the new bridge structure. A significant seismic event may require additional supports counter act the liquefication.

Appendix

Figure 4
Boring Locations -
Provo River Bridge Replacement
Provo-Orem Transportation
Improvement Project

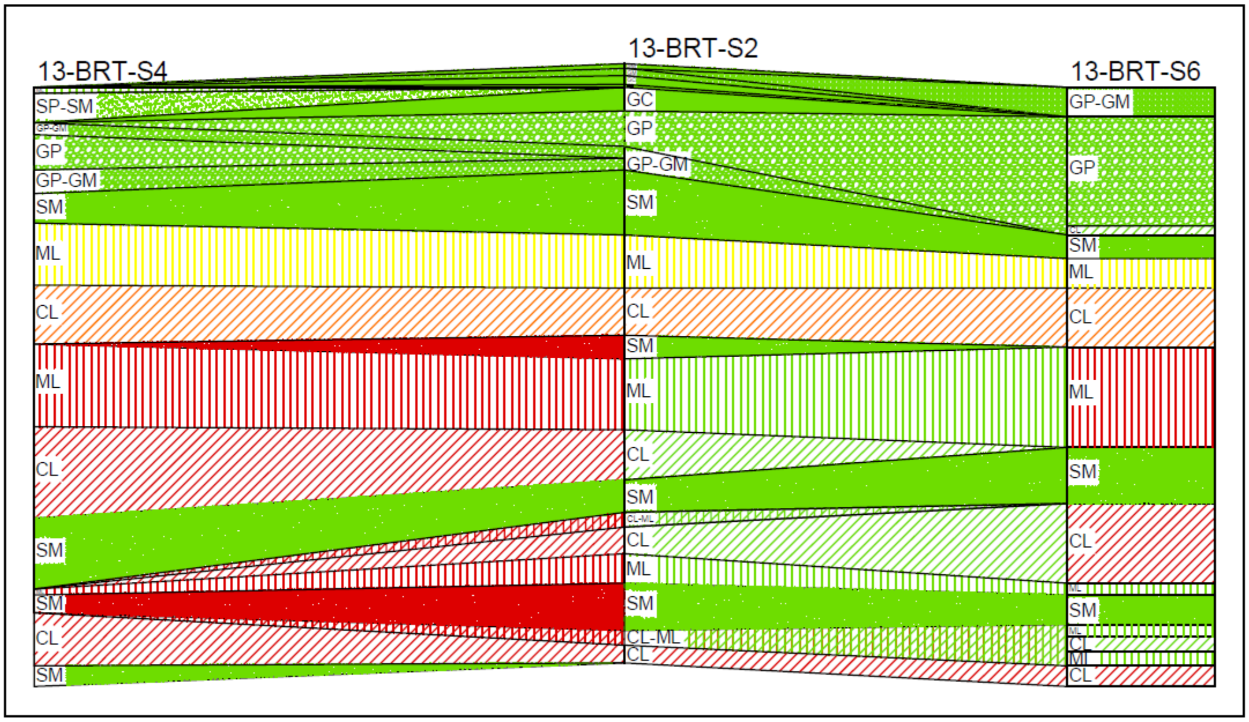
13-BRT-S4
13-BRT-S2
13-BRT-S6
SP-SM
GP
GP-GM
SM
ML
CL
ML
CL
SM
SM
CL
SM
GC
GP
GP-GM
SM
ML
CL
SM
ML
CL
SM
CL
ML
SM
CL-ML
CL
GP-GM
GP
SM
ML
CL
ML
SM
CL
SM
CL
ML
CL

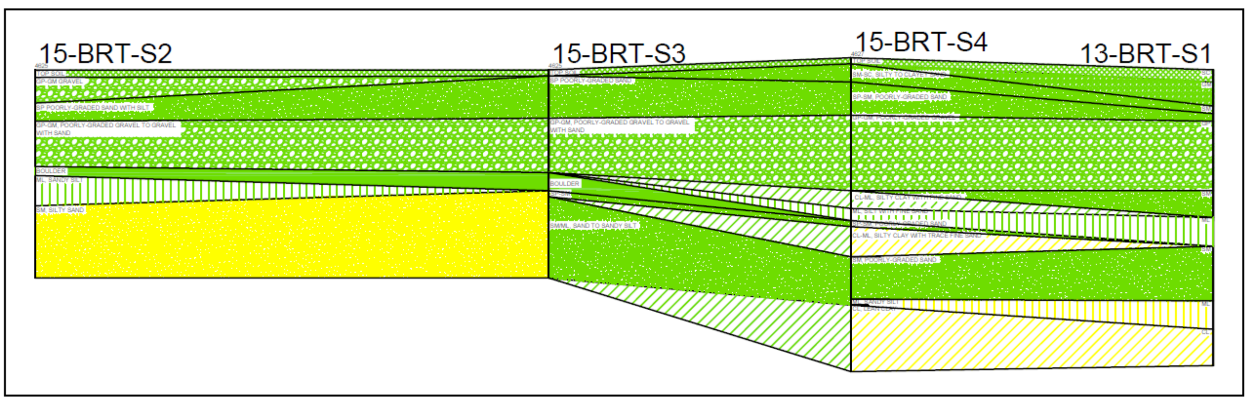
15-BRT-S2
15-BRT-S3
15-BRT-S4
13-BRT-S1

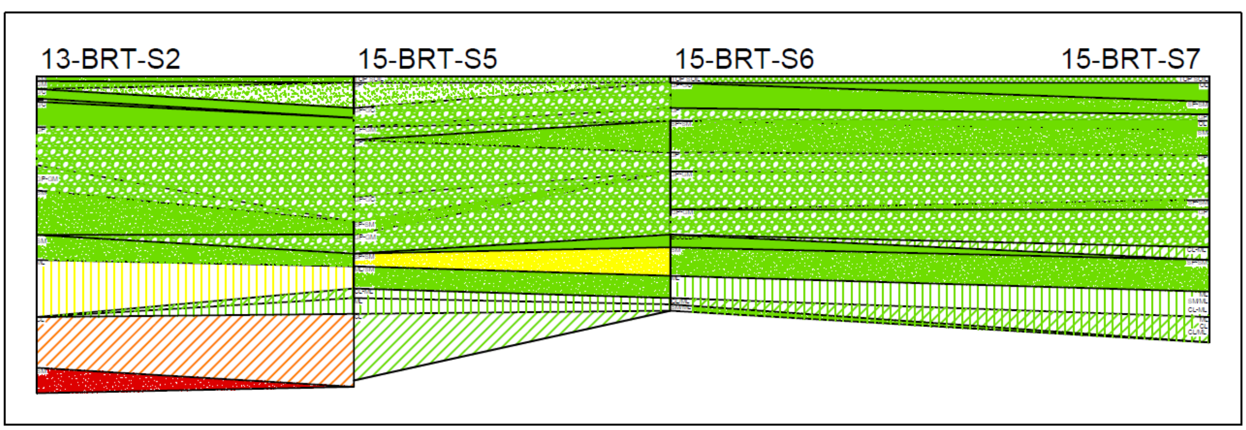
13-BRT-S2
15-BRT-S5
15-BRT-S6
15-BRT-S7

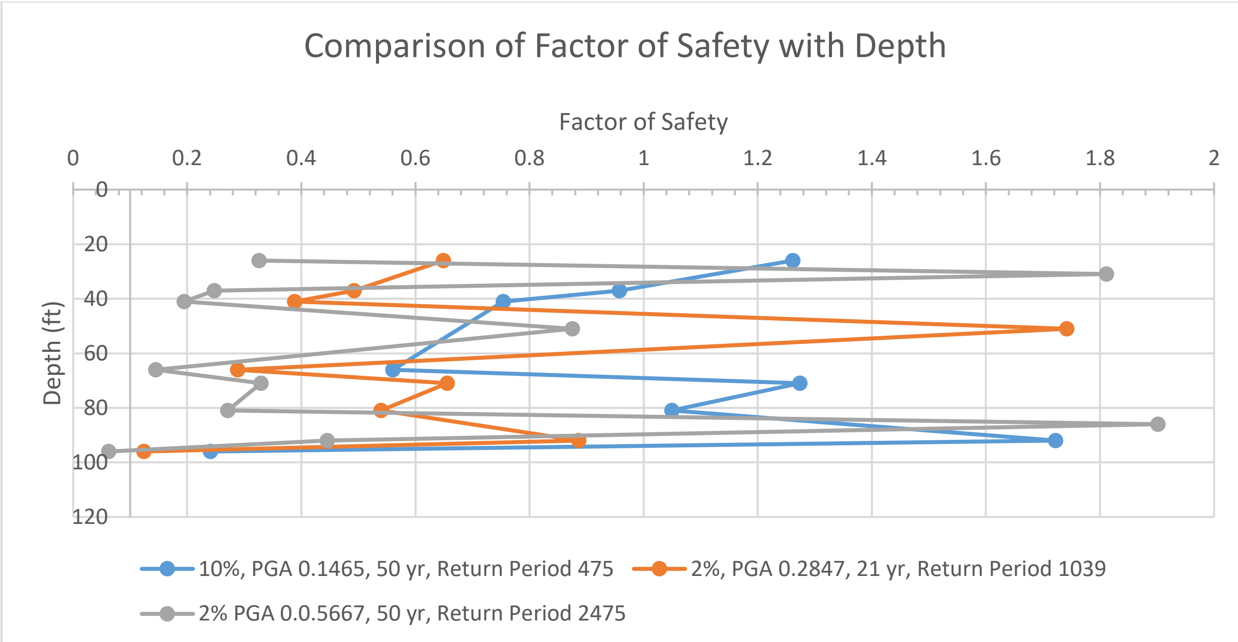

13 BRT S-1

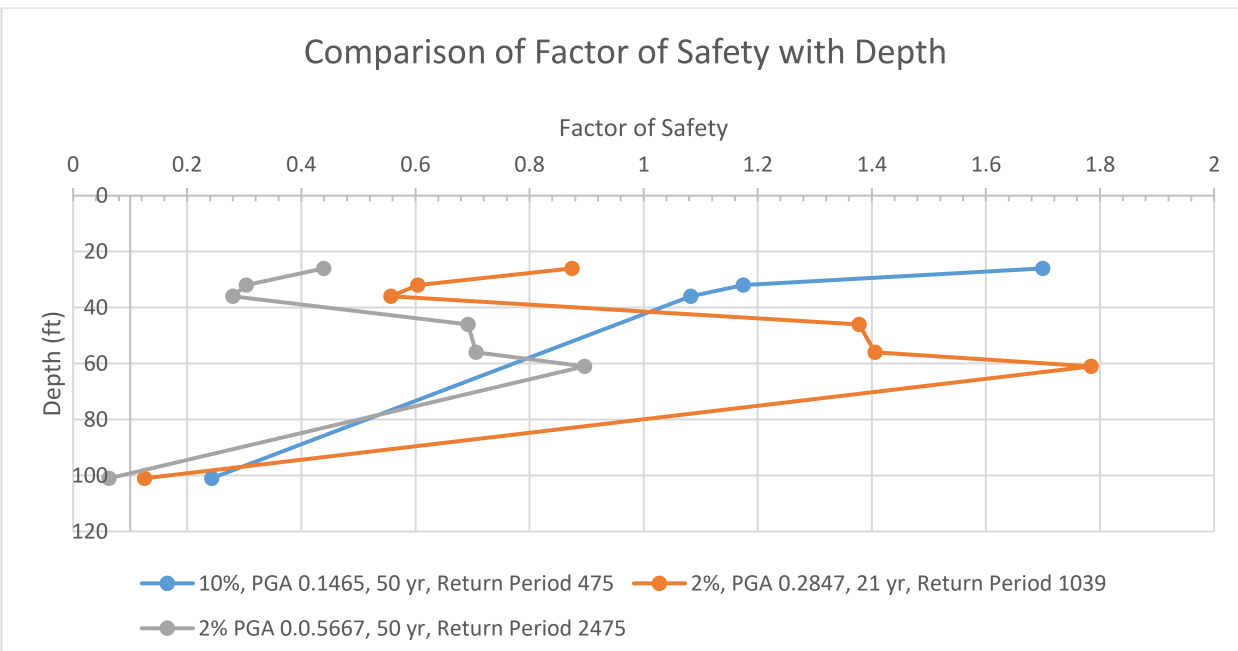

13 BRT S2

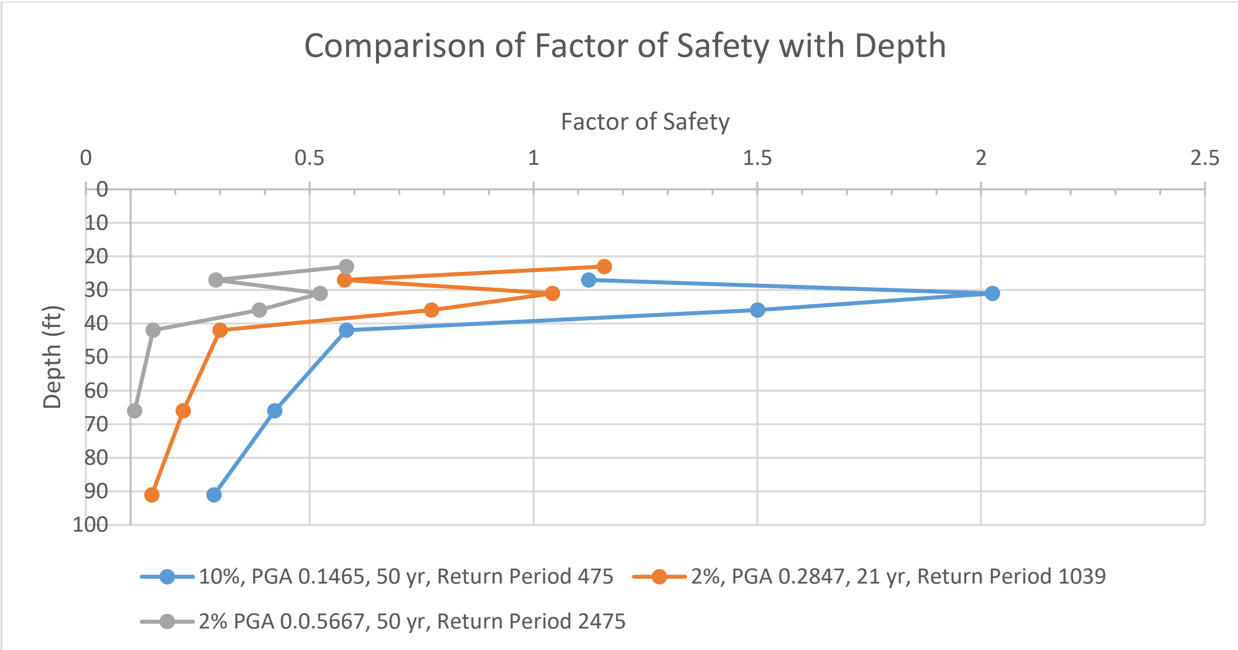

13 BRT S3

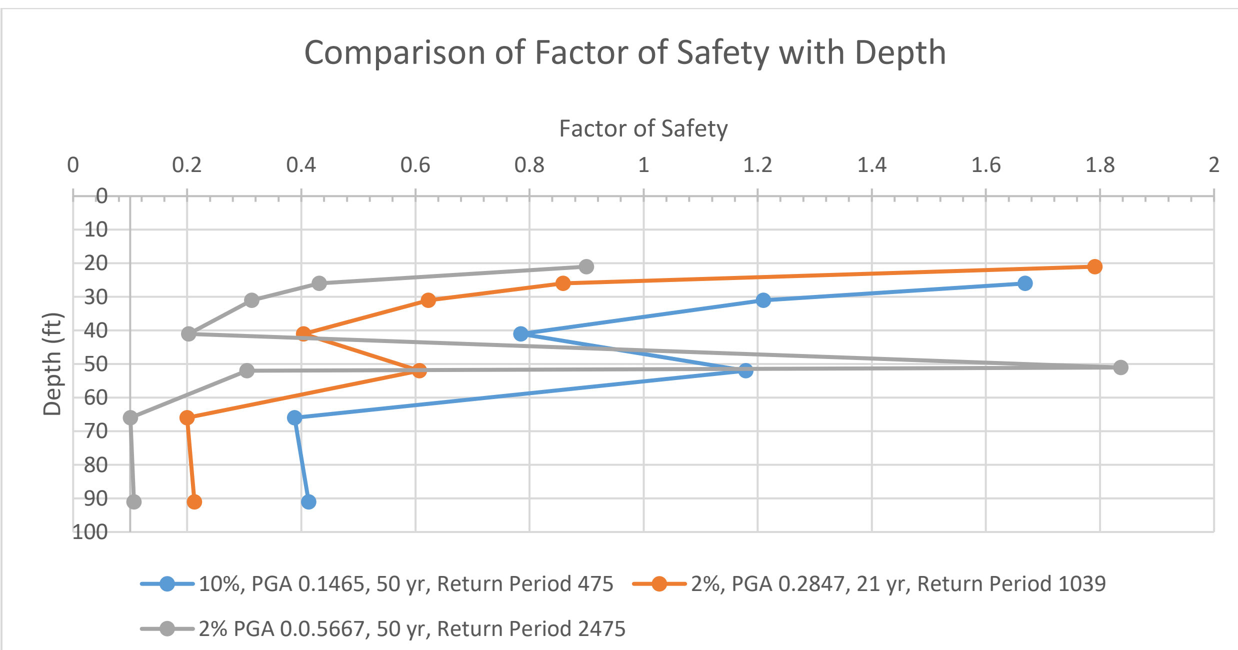

13 BRT S4

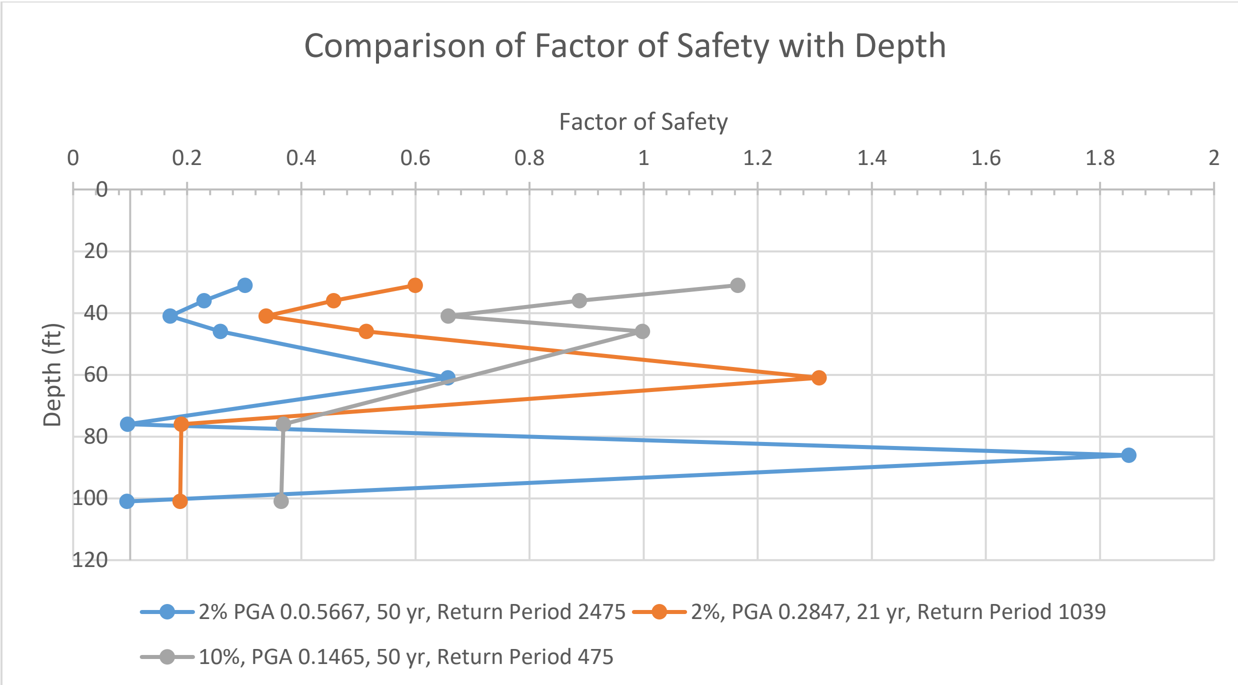

13 BRT S5

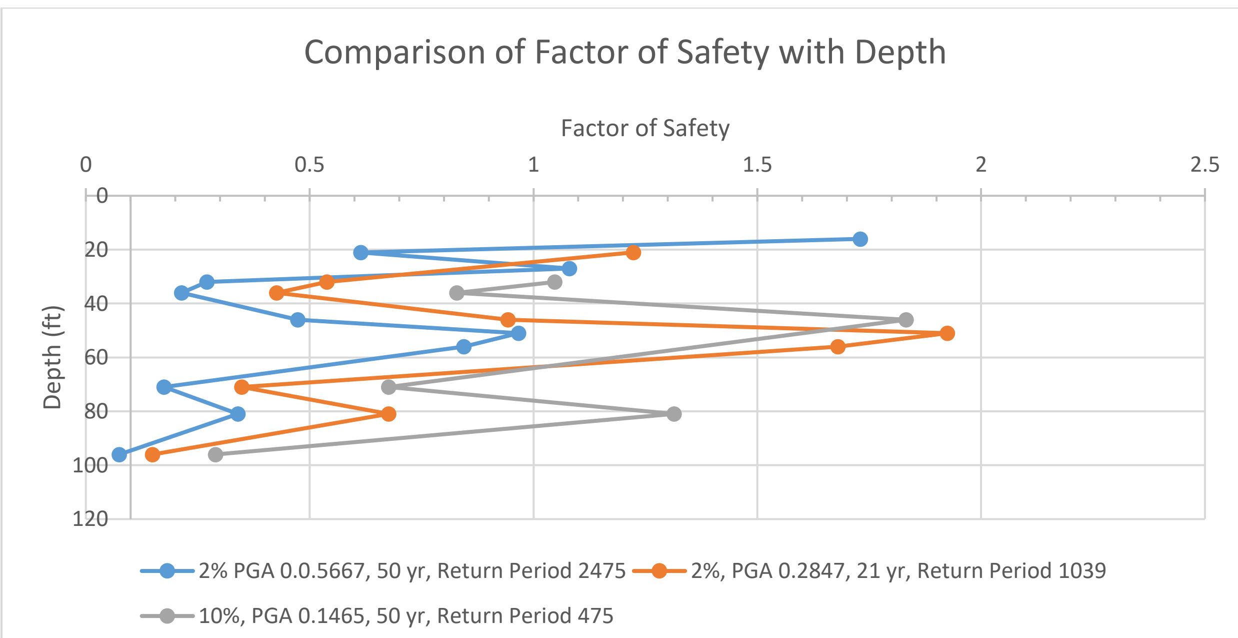

13 BRT S6

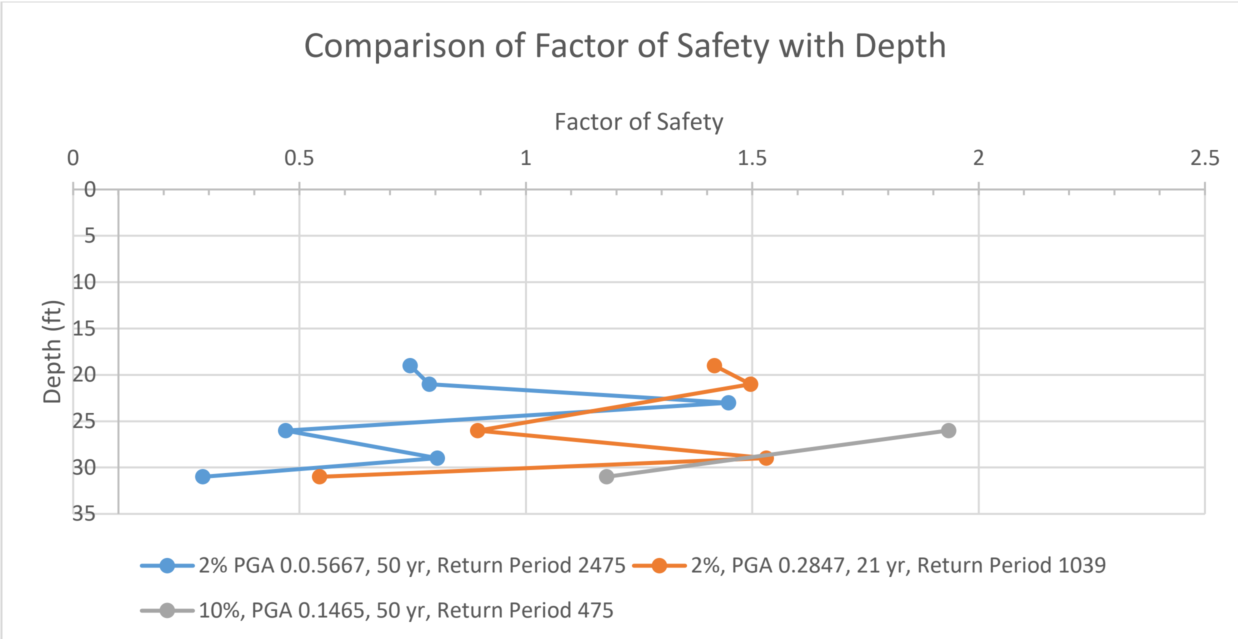

15 BRT S2

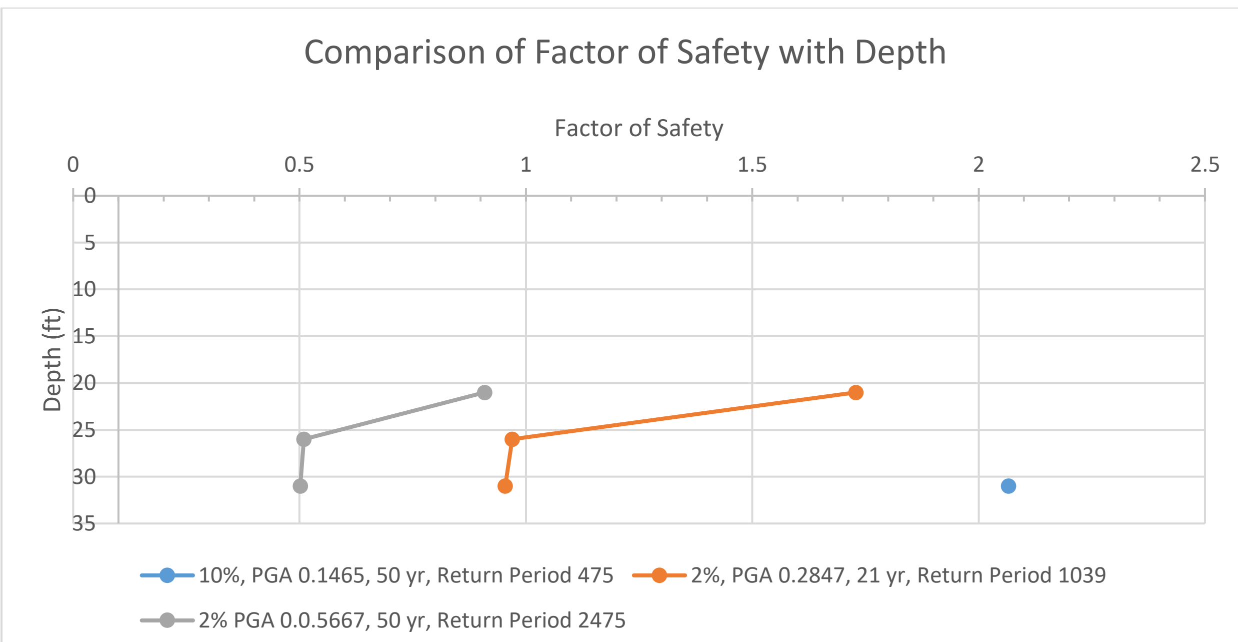

15 BRT S3

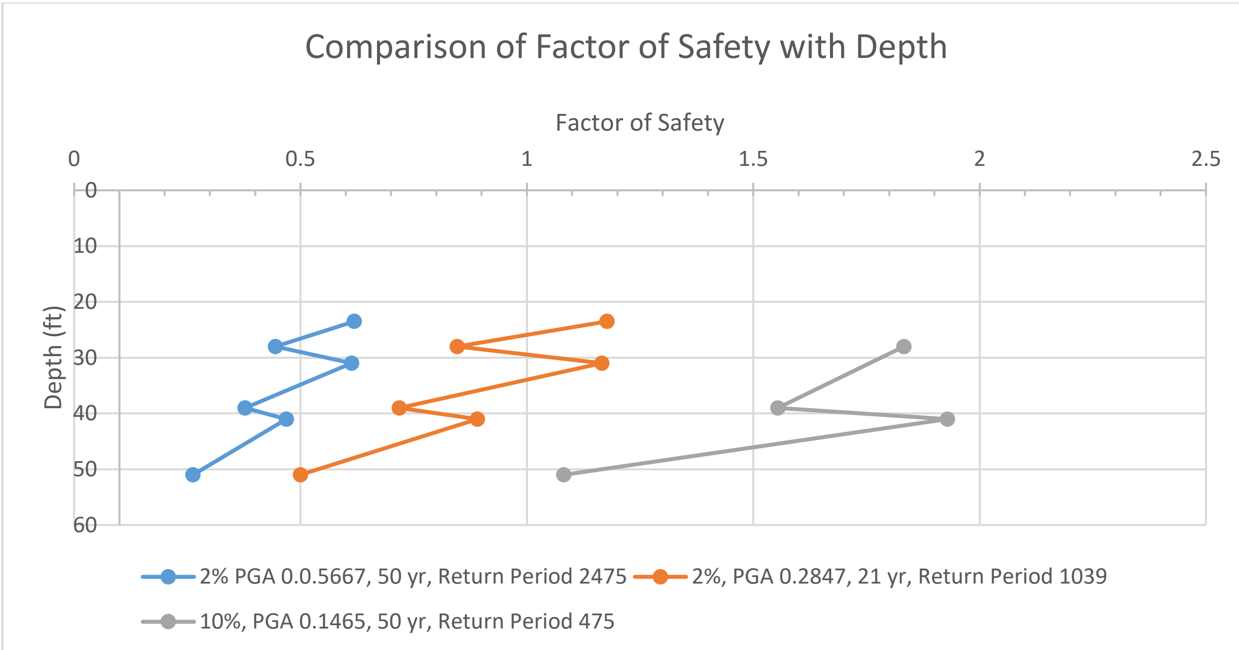

15 BRT S4

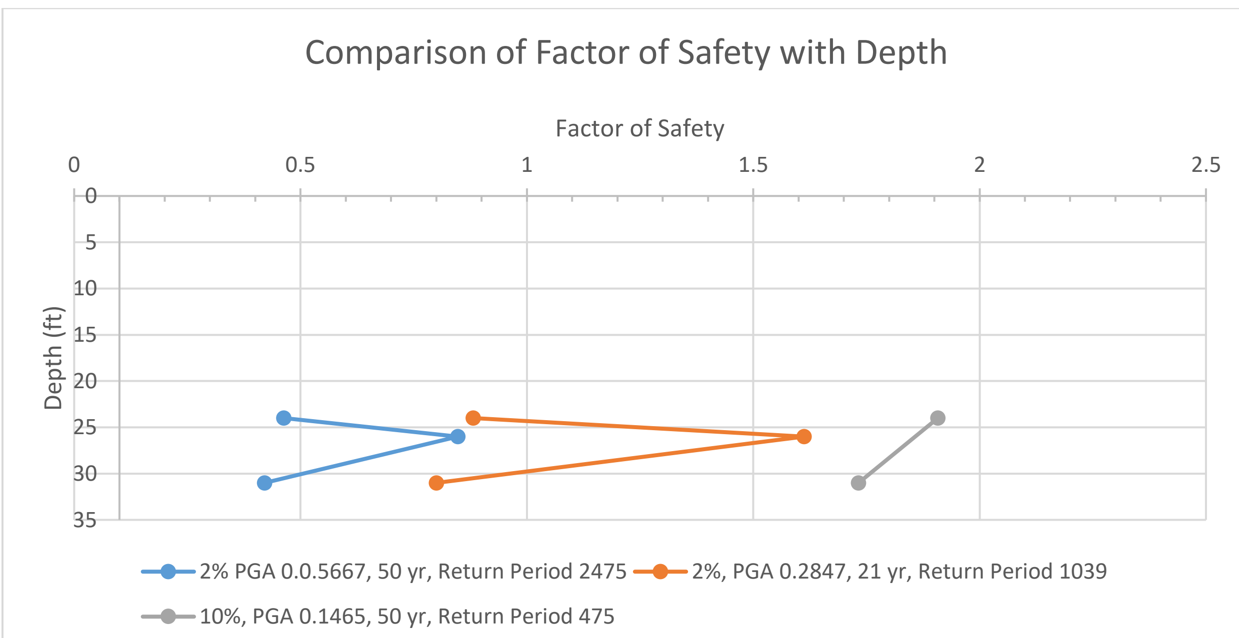

15 BRT S5

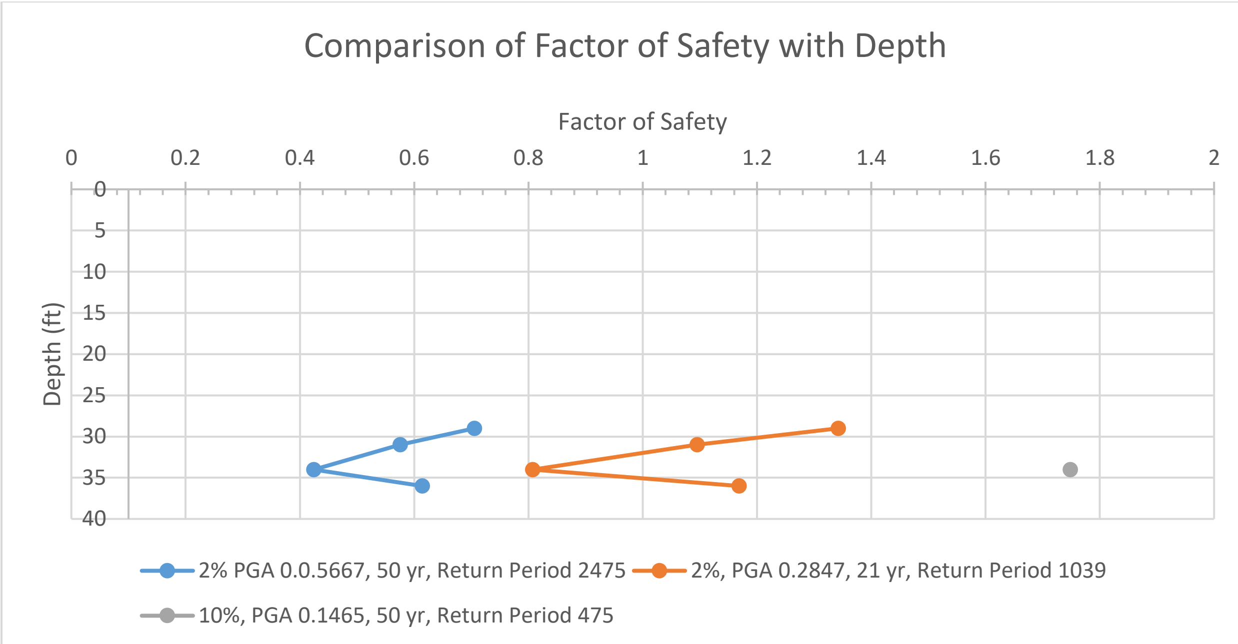

15 BRT S6

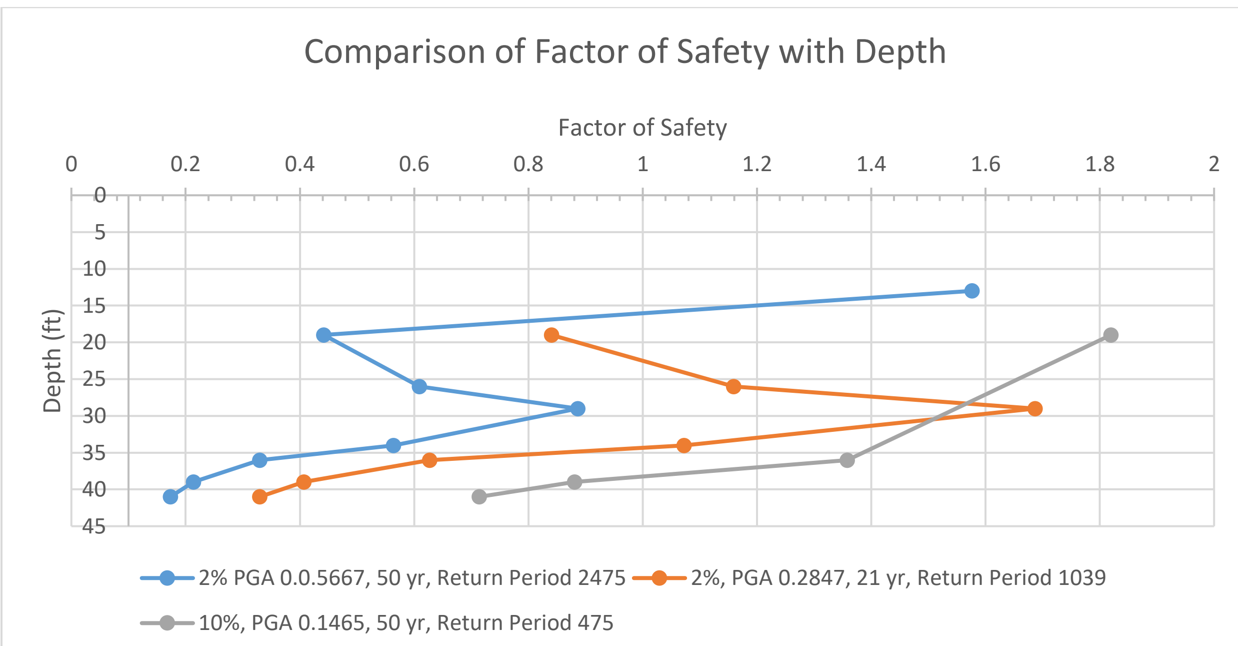

15 BRT S7